 Erosion and Sediment Yields in the Changing Environment (Proceedings of a symposium held at the Institute of Mountain Hazards and Environment, CAS-Chengdu, China, 11–15 October 2012) (IAHS Publ. 356, 2012).

Characteristics of runoff processes on unmetalled loess roads under experimental rainfall conditions

FENGXIA TIAN[1], XIUBIN HE[1], GUIYU LI[2] & SHIQING ZHENG[3]

1 Key Laboratory of Mountain Surface Processes and Ecological Regulation, Institute of Mountain Hazards and Environment, Chinese Academy of Sciences, Chengdu 610041, China
tianfengxia@imde.ac.cn
2 CHINA Water Resources Pearl River Planning, Surveying and Designing Co. Ltd, Guangzhou 510610, China
3 Institute of Soil and Water Conservation, CAS & MWR, Yangling, Shaanxi 712100, China

Abstract Runoff commonly triggers severe erosion on unmetalled road surfaces and roadside slopes. In this context, this paper explores the use of theoretical analysis of runoff processes for an unmetalled loess road, based on the kinematic wave theory, and explores the key controlling factors. The results of the theoretical analysis are assessed using measured data from simulated rainfall tests on artificial experimental road sections. The results suggested that: (1) the kinematic wave equation is appropriate for describing dynamic processes of overland flow on unmetalled loess roads; (2) the discharge, depth and velocity of runoff on the unmetalled loess roads increased with increasing rainfall intensity, whereas the velocity of runoff increased with increasing slope length; (3) the velocity of runoff increased as flow depth decreased with increasing slope gradient; and (4) unit width discharge on road sections with different slopes under the same rainfall intensity (120 mm h^{-1}) remained similar.

Keywords unmetalled loess roads; kinematic wave theory; flow depth; flow velocity; slope gradient

INTRODUCTION

Numerous unmetalled or unpaved earth roads have been constructed recently on the hill slopes of the Loess Plateau in China. The surfaces of these roads are primarily composed of loess and are, therefore, almost totally free of any paving. Furthermore, many of these roads are severely compacted, and therefore have higher soil bulk densities and lower infiltration rates than the surrounding soil as a result of trafficking. These features provide important arterial routes for overland flow. With increasing trafficking, such roads are experiencing progressively severe erosion and loss of soil, with quantitative estimates ranging between 10 000 and 100 000 t km^{-2} $year^{-1}$ (Zheng *et al*., 2004, 2005).

Previous studies have shown that peak flow in a watershed increased significantly due to road construction (Thomas & Megahan, 1998) and that approximately 90% of the sediment yield from forest areas in North Carolina, USA, resulted from road erosion (Hoover, 1952). In the Loess Plateau area of China, although roadways account for only 1% of the area of the Yangou watershed, they contribute 42.3% of the total sediment export (Xu *et al*., 2008). To date, however, there have been relatively few studies examining erosion processes and mechanics on unmetalled roads (Zheng *et al*., 1994; Cao *et al*., 2006; Shi *et al*., 2009; Liu *et al*., 2010) especially with respect to overland flow hydraulics and sediment yield processes (Ziegler *et al*., 2001; Tian *et al*., 2009).

On the Chinese Loess Plateau, overland runoff originating from rainfall is the main driver for soil erosion on hillside unmetalled roads (Zheng *et al*., 2004, 2009; Liu *et al*., 2010). The dynamic processes of slope erosion are strongly related to the hydraulic characteristics of surface runoff, including flow discharge, velocity and water depth (Julien & Simons, 1985). Thus, it is important to study the characteristics of runoff processes on hillside unmetalled roads in this region in order to have an improved understanding of erosion processes and their key controls. Existing models of runoff processes typically employ the kinematic wave approximation to the Saint Venant flow equations (Howes *et al*., 2006) and these kinematic representations of overland flow comprise both continuity and momentum equations.

Given the above context, the aim of this work was to study the characteristics of overland flow on unmetalled loess roads and to improve understanding of the key controlling factors on the basis of the kinematic wave theory. On this basis, the work assessed whether the kinematic wave

equation is appropriate for describing the dynamic processes of overland flow on unmetalled loess roads and verified the results of the theoretical analysis using measured data from simulated rainfall tests on artificial road sections. It was intended that the findings would provide basic data for informing road construction in the Loess Plateau region and contribute to the subsequent development of improved erosion models for hillside unmetalled roads.

THE KINEMATIC MODEL

Overland flow dynamics

The kinematic wave equations for overland flow consist of continuity and momentum equations (Woolhiser & Liggett 1967; Eagleson, 1970):

$$\frac{\partial h}{\partial t}+v\frac{\partial h}{\partial x}+h\frac{\partial v}{\partial x}=q^{*} \tag{1}$$

$$\frac{\partial v}{\partial t}+v\frac{\partial v}{\partial x}+g\frac{\partial h}{\partial x}=g\left(S_0-S_f\right)-q^{*}\frac{v}{h} \tag{2}$$

where h is flow depth (cm), v is flow velocity (cm h^{-1}), q^{*} is the excess rainfall rate (cm h^{-1}), S_f is friction slope (cm cm^{-1}), S_0 is bed slope (cm cm^{-1}), g is the gravity acceleration (cm s^{-2}), t is time (h), and x is distance (cm).

In addition, the kinematic wave approximation is one of the popular approximations to the full Saint-Venant equations. Assuming that the friction slope is equated to the bed slope in the momentum equation, (2). Equations (1) and (2) reduce to:

$$\frac{\partial h}{\partial t}+v\frac{\partial h}{\partial x}+h\frac{\partial v}{\partial x}=q^{*} \tag{3}$$

$$S_f=S_0 \tag{4}$$

where S_f is described by the Manning equation and the unit width discharge (q, cm^2 h^{-1}) can be expressed as:

$$q=\frac{1}{\eta}h^{5/3}S_0^{1/2}=\frac{1}{\eta}h^{5/3}\cos^{1/2}\theta\sin^{1/2}\theta \tag{5}$$

where η is the Manning roughness coefficient and θ is slope gradient (°).

Runoff processes

When rainfall intensity is I (cm h^{-1}), the excess rainfall rate (q^{*}) on a surface of slope θ can be described as:

$$q^{*}=I\cos\theta-f_i \tag{6}$$

where f_i is the infiltration rate (cm h^{-1}).

Unit width discharge (q) at distance l (cm) from the top of the slope, can be calculated on the basis of:

$$q=\int_0^{l}q^{*}dx=\left(I\cos\theta-f_i\right)l \tag{7}$$

Again, assuming that the flow depth is h and flow velocity is v, at distance l from the top of the slope, q can be described as:

$$q=vh=\left(I\cos\theta-f_i\right)l=\frac{1}{\eta}h^{5/3}\cos^{1/2}\theta\sin^{1/2}\theta \tag{8}$$

Therefore, h and v can be expressed as:

$$h = \frac{\left[\eta\left(I\cos\theta - f_i\right)l\right]^{0.6}}{\cos^{0.3}\theta\sin^{0.3}\theta} \tag{9}$$

$$v = \eta^{-0.6}\left[\left(I\cos\theta - f_i\right)l\right]^{0.4}\cos^{0.3}\theta\sin^{0.3}\theta \tag{10}$$

Assuming that the infiltration rate (f_i) of the unmetalled loess roads is negligible, equations (7), (9) and (10) can be simplified to the following equations (Zheng *et al*., 1994; Tian *et al*., 2009):

$$q = Il\cos\theta \tag{11}$$

$$h = \frac{\left(\eta Il\right)^{0.6}\cos^{0.3}\theta}{\sin^{0.3}\theta} \tag{12}$$

$$v = \eta^{-0.6}\left(Il\right)^{0.4}\cos^{0.7}\theta\sin^{0.3}\theta \tag{13}$$

Derivatives of $\frac{dv}{d\theta}$ can be calculated as：

$$\frac{dv}{d\theta} = \eta^{-0.6}\left(Il\right)^{0.6}\left(0.3\sin^{-0.7}\theta\cos^{1.7}\theta - 0.7\sin^{1.3}\theta\cos^{-0.3}\theta\right) \tag{14}$$

MATERIALS AND METHODS

Experimental design and observations

The rainfall simulation experiments were conducted at the State Key Laboratory of Soil Erosion and Dryland Farming on the Loess Plateau in Yangling, China. A rainfall simulator projected a spray of tap water from a height of 16 m to produce a simulated rainstorm at a controllable intensity. The artificial unmetalled loess road sections were created by packing loess soil (collected from Yan'an in Shaanxi located in the northern part of the Loess Plateau) into metal boxes, 2.0 m in length, 0.55 m in width, and 0.35 m in depth (Fig. 1). The soil was packed uniformly into the boxes in six 5-cm layers to a depth of 30 cm with a corresponding bulk density of 1.35 g cm^{-3}. Twelve soil boxes were prepared and the bottoms of the boxes were perforated and covered with a single layer of gauze to facilitate even drainage of percolating soil water. Runoff was funnelled to a collection vessel placed at the lower end of the box.

Fig. 1 The artificial unmetalled loess road sections, showing flow velocity measurement using a dye tracing technique.

The experimental design consisted of 10 treatments comprising five different slope gradients (6°, 9°, 12°, 15° and 18°) under the same rainfall intensity (120 mm h^{-1}), and five different rainfall intensities (60 mm h^{-1}, 90 mm h^{-1}, 120 mm h^{-1}, 150 mm h^{-1} and 180 mm h^{-1}) under the same slope (15°) with two replications of each treatment. A simulated rainstorm was applied for 60 minutes. Runoff samples were collected continuously throughout the simulated storm at 3 minute intervals and the volume recorded. The samples were oven dried at 105°C and subsequently weighed to determine sediment content for estimating export from the artificial road sections. Flow velocity was measured at 3 minute intervals from the commencement of runoff using dye tracers along five separate 40-cm long sections, evenly spaced from the upper to the lower ends of the slope (Fig. 1).

Data processing

After runoff was determined to have reached steady state, the values of the measured velocities, taken three times for each experimental section, were averaged to estimate the mean flow velocity. The measured mean velocity was multiplied by a correction factor of 0.67 to correct for the interaction of the dye and the runoff (Li *et al*., 1996).

Flow depth is an important aspect of the hydraulic characteristics of surface runoff. However, it was difficult to measure accurately the flow depth on the experimental road sections due to the very thin layer of water and the changing conditions of the soil surface. Accordingly, the flow depth (h cm) was calculated using the following equation and assuming that overland flow on the experimental road sections was evenly distributed along the slope:

$$h = \frac{Q}{vbt} \tag{15}$$

where v is the mean flow velocity (cm s^{-1}), b is the width of road sections (cm), t is the sampling interval (s) and Q is the collected runoff volume (mL).

RESULTS AND DISCUSSION

Application of kinematic wave theory to runoff on the unmetalled loess roads

Woolhiser & Liggett (1967) normalized the above momentum equation (2) to simplify overland flow investigations and defined the kinematic flow number $K = \frac{S_0 L}{F_{r0}^2 H_0}$ (S_0 is bed slope, L is slope length, F_{r0} and H_0 are the Froude number and flow depth at the downstream end of the slope, respectively). This work suggested that the kinematic wave approximation is suitable for overland flow when K is greater than 10. Morris & Woolhiser (1980) introduced the additional criterion that combines F_{r0} and K and reported that the kinematic wave approximation performed well when $F_{r0}^2 K > 5$.

In our study, values of the kinematic flow number (K) ranged from 18.82 to 65.35 while $F_{r0}^2 K$ ranged from 433.26 to 5145.21 (Table 1). These results suggested that it is appropriate to describe the dynamic processes of runoff on unmetalled loess roads using the kinematic wave equation.

Table 1 Mean values of K and $F_{r0}^2 K$ of surface runoff on the unmetalled loess roads.

	Rainfall intensity (mm·h^{-1})					Slope gradient (°)				
	60	90	120	150	180	6	9	12	15	18
K	65.35	38.41	35.94	23.71	20.14	59.28	41.71	26.84	23.71	18.82
$F_{r0}^2 K$	5145.21	2476.37	611.94	476.13	433.26	548.61	567.06	701.54	747.69	756.38

Theoretical analysis of runoff processes on unmetalled loess roads

Upland areas generally provide a significant source of water for surface runoff. Flow depth and velocity on slopes determine runoff erosivity and sediment transport capacity (Carson & Kirkby, 1972). Therefore, knowledge of surface runoff is essential for estimating soil losses from unmetalled roads.

It is noticeable from equations (11) and (13) that unit width discharge (q), flow depth (h) and flow velocity (v) increase with increasing rainfall intensity (I) and slope length (L), while q and h decrease with increasing slope gradient. The influence of slope gradient (θ) on flow velocity is not obvious and cannot be expressed as a simple linear function. Additionally, since $\cos\theta = 0.8367$ and thus $\theta = 33.21°$ assuming that $\frac{dv}{d\theta} = 0$ in equation (14), the flow velocity (v) on a slope reaches its maximum value at a slope gradient of 33.21°. On this basis, v firstly increases and then decreases with increasing slope gradient.

Runoff processes on unmetalled loess roads

The mean flow velocity of each experimental umetalled road section, under each of the simulated rainfall conditions, increased with increasing distance from the upper slope (Fig. 2). As an example, the flow velocity at the lower end of the unmetalled loess road section, at a slope of 15° and rainfall intensity of 60 mm h^{-1}, was 2.67 times that at the upper edge.

The unit width discharge of each sampling interval on the 15° road sections increased with increasing rainfall intensity (Fig. 3). In contrast, the unit width discharge of each sampling interval

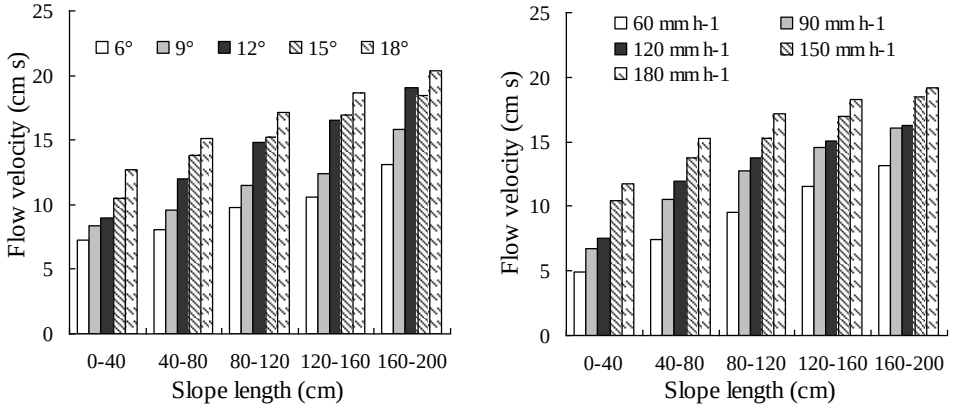

Fig. 2 Flow velocity of each 40-cm long section from the upper to the lower ends of the slope.

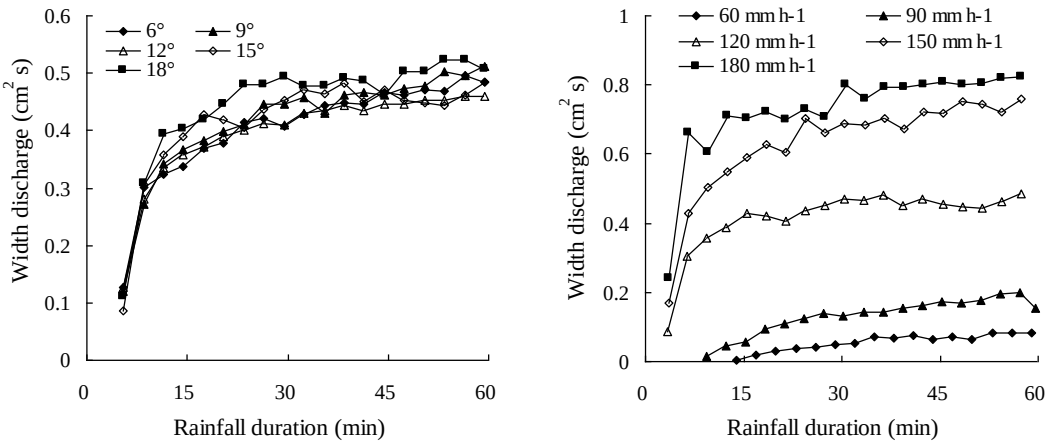

Fig. 3 Variation of unit width discharge over time under the different slope and rainfall intensity conditions.

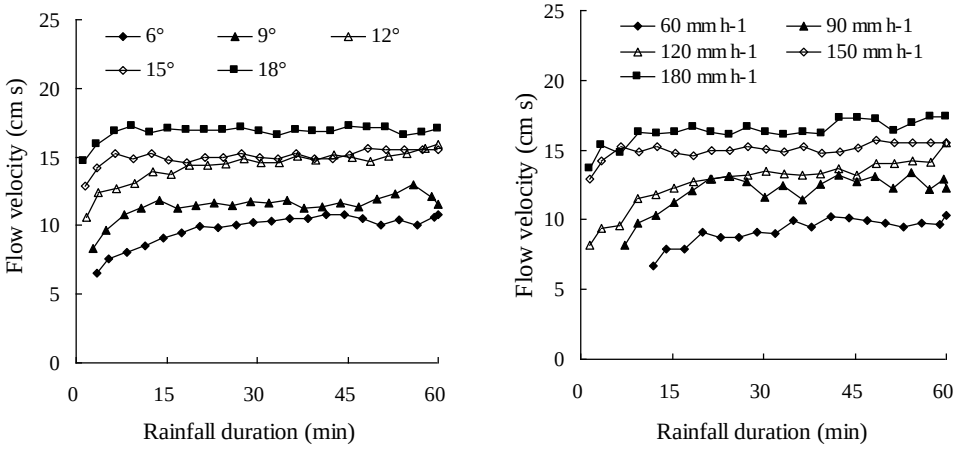

Fig. 4 Variation of flow velocity over time under the different slope and rainfall intensity conditions.

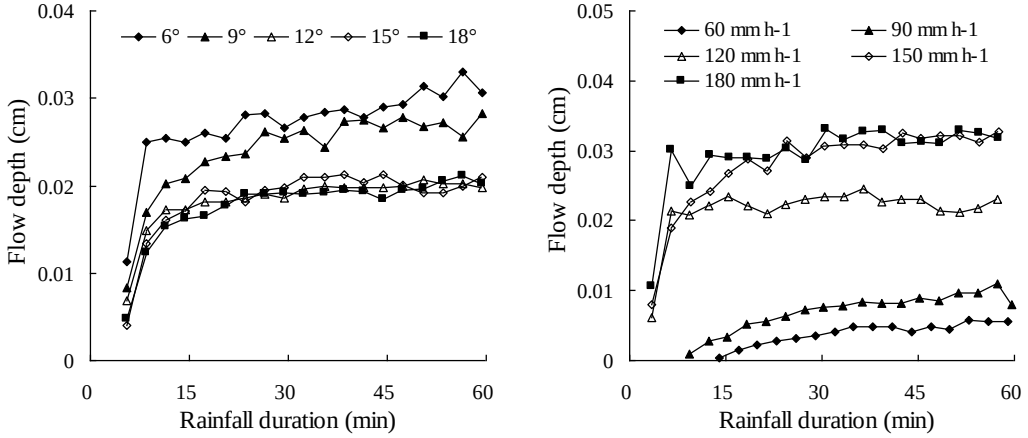

Fig. 5 Variation of flow depth over time under the different slope and rainfall intensity conditions.

on the alternative slope road sections differed less but increased over the duration of rainfall. Accordingly, at the beginning of runoff, the unit width discharge was only 0.08 $cm^2\ s^{-1}$ while at the end of the simulated rainfall event it was 0.51 $cm^2\ s^{-1}$ (Fig. 3).

Flow velocity and depth on the unmetalled loess road sections both increased with increasing rainfall intensity, and flow velocity increased with increasing slope gradient (Figs 4 and 5). In contrast, with this pattern, flow depth decreased with increasing slope gradient (left-hand plot in Fig. 5).

CONCLUSIONS

This study demonstrated that the kinematic wave equation is appropriate for describing dynamic runoff on unmetalled loess roads. Theoretically, unit width discharge, flow depth and flow velocity increase with increasing rainfall intensity and slope length, while unit width discharge and flow depth decrease with increasing slope gradient. In addition, flow velocity first increases and then decreases with increasing slope gradient, with the critical threshold value for this change being 33.21°. In comparison with these theoretical observations, the measured unit width discharge, flow velocity and flow depth of each sampling interval on the experimental road sections under the different rainfall intensity conditions increased with increasing rainfall intensity, while flow depth almost decreased with increasing slope gradient. These experimental observations are therefore

consistent with the theoretical analysis. The measured flow velocity on the experimental road sections increased with increasing slope gradient because the maximum slope of these road sections was only 18°. In addition, the unit width discharge on the different slope experimental road sections under the same rainfall intensity (120 mm h^{-1}) remained similar, implying that rainfall intensity is the most important factor governing surface runoff processes.

Acknowledgements Thanks are extended to Prof. Zhanli Wang and Ms Chunyan Ma, of the Institute of Soil and Water Conservation for their help with the experiment. Thanks are also extended to Prof. Xinbao Zhang for his help in finishing this paper. The draft paper benefitted from editorial review.

REFERENCES

Cao, C. S., Chen, L., Gao, W., Chen, Y. & Yan, M. (2006) Impact of planting grass on terrene roads to avoid soil erosion. *Landscape Urban Plan*. 78(3), 205–216.

Carson, M. A. & Kirkby, M. J. (1972) *Hillslope Form and Process*. Cambridge University Press, New York.

Eagleson, P. S. (1970) *Dynamic Hydrology*. McGraw-Hill, Inc., New York.

Hoover, M. D. (1952) Water and timber management. *J. Soil and Water Conservation* 7(4), 75–78.

Howes, D. A., Abrahams, A. D. & Pitman, E. B. (2006) One- and two-dimensional modelling of overland flow in semiarid shrubland, Jornada basin, New Mexico. *Hydrol. Processes* 20, 1027–1046.

Julien, P. Y. & Simons, D. B. (1985) Sediment transport capacity of overland flow. *Trans. ASAE* 28(3), 755–762.

Li, G., Abrahams, A.D. & Atkinson, J. F. (1996) Correction factors in the determination of mean velocity of overland flow. *Earth Surf. Proc. Land.* 21(6), 509–515.

Liu, G., Tian, F. X., Warrington, D. N., Zheng, S. Q. & Zhang, Q. (2010) Efficacy of grass for mitigating runoff and erosion from an artificial loessial earthen road. *Trans. ASABE* 53(1), 119–125.

Morris, E. M. & Woolhiser, D. A. (1980) Unsteady one-dimensional flow over a plane: Partial equilibrium and recession hydrographs. *Water Resour. Res.* 16, 355–360.

Shi, Z. H., Chen, L. D., Yang, C. C., Yan, F. L. & Peng, Y. X. (2009) Soil loss and runoff processes on unpaved road from rainfall simulation tests in the Three Gorges Area, China. *Acta Ecologica Sinica* 29(12), 6785–6792 (in Chinese with English abstract).

Thomas, R. B. & Megahan, W. F. (1998) Peak flow responses to clear-cutting and roads in small and large basins, western Cascades, Oregon: A second opinion. *Water Resour. Res.* 34(12), 3393–3403.

Tian, F. X., Liu, G., Zheng, S. Q., Ma, C. Y. & Zhang, Q. (2009) Influence of herbaceous plants on runoff hydraulic characteristics and sediment generation on terrene roads. *Trans. CSAE* 25(10), 25–29 (in Chinese with English abstract)

Woolhiser, D. A. & Liggett, J. A. (1967) Unsteady one-dimensional flow over a plane – the rising hydrograph. *Water Resour. Res.* 3(3), 753–771.

Xu, X. X., Ju, T. J. & Zheng, S. Q. (2008) Sediment sources analysis of the Yangou watershed under a certain rainstorm event in the hilly-gully region of loess plateau. *Science of Soil and Water Conservation* 6(3), 38–42 (in Chinese with English abstract).

Zheng, S. Q., Zhou, B. L. & Zhao, K. X. (1994) Valley-slope road erosion and its control measures in Wangdong gully experimental area located in Changwu county. *J. Soil and Water Conservation* 8(3), 29–35 (in Chinese with English abstract).

Zheng, S. Q., Huo, J. L. & Li, Y. (2004) Hilly road erosion and control on Loess Plateau region. *Bulletin of Soil and Water Conservation* 24(1), 46–48 (in Chinese with English abstract).

Zheng, S. Q., Wen, J. Y. & Yin, Z. J. (2005) Anti-erosive mechanism and technology of productive biological road of loess hillside. *Res. Soil Water Cons.* 12(5), 95–97 (in Chinese with English abstract).

Zheng, S. Q., Tian, F. X., Wang, Z. L. & Xu, X. X. (2009) Comparison tests on runoff and sediment yield process from earth road and plant-covered road in loess hilly region. *Journal of Sediment Res.* 4, 1–6 (in Chinese with English abstract).

Ziegler, A. D., Giambelluca, T. W., Sutherland, R. A., *et al.* (2001) Contribution of Horton overland flow to runoff on unpaved mountain roads in northern Thailand. *Hydrol. Processes* 15, 3203–3208.